Phys Chem Minerals (2005) 32: 290–294
DOI 10.1007/s00269-005-0467-6

ORIGINAL PAPERS

H. Kojitani · M. Kido · M. Akaogi

Rietveld analysis of a new high-pressure strontium silicate $SrSi_2O_5$

Received: 1 July 2004 / Accepted: 2 March 2005 / Published online: 14 May 2005

Abstract High-pressure synthesis of a new $SrSi_2O_5$ phase was performed at 16 GPa and 900°C by using a Kawai-type multianvil apparatus. The powder X-ray diffraction pattern of the compound was analyzed by Rietveld refinement based on the structure of a high-pressure polymorph of $BaGe_2O_5$, $BaGe_2O_5$ III. The structure is orthorhombic with space group *Cmca* and cell parameters of a = 5.2389(1) Å, b = 9.2803(2) Å, c = 13.4406(1) Å, V = 653.46(2) Å^3 (Z = 8, ρ_{calc} = 4.549 g/cm^3). The structure consists of layers containing SiO_6 octahedra and SiO_4 tetrahedra. In a unit layer, oxygen and strontium atoms are arranged in an approximation to hexagonal close-packing. The strontium atom is accommodated in a 12-coordinated site. Each SiO_6 octahedron shares four corners with SiO_4 tetrahedra and the other two corners with another SiO_6 octahedra. The SiO_6 octahedra are linked to each other to form SiO_6 chains along the a-axis. This is the first known example of a silicate with a $BaGe_2O_5$ III-type structure.

Keywords Strontium silicate · Barium germanate · Calcium silicate · Rietveld analysis · High pressure

Introduction

Since Sr is an alkaline-earth metal element like Mg and Ca and has a slightly larger ionic radius than Ca, it is interesting to examine the substitution of Sr for Ca in Ca-based structures from the crystal chemistry point of view. Especially, strontium metasilicate, $SrSiO_3$, is a potentially good analog of $CaSiO_3$ which is one of the major endmember components in the constituent minerals of the Earth's crust and mantle. The high-pressure phase relations of $SrSiO_3$ were investigated by Shimizu et al. (1970) and Fleischer and DeVries (1988). In particular, Shimizu et al. (1970) reported the results of high-pressure experiments up to 12 GPa, based on the pressure scales of those days. According to their results, pseudowollastonite-type $SrSiO_3$ ($SrSiO_3$ I), which is stable at 1 atm, transforms to $SrSiO_3$ II at about 3.5 GPa and to $SrSiO_3$ III at about 6 GPa. The structure of $SrSiO_3$ II was determined to be a walstromite-type structure and that of $SrSiO_3$ III to contain four-membered tetrahedra rings (Machida et al. 1982). In our high-pressure experiments in the SrO–SiO_2 system to research phase relations of $SrSiO_3$ at higher pressure, it has been found that $SrSiO_3$ III decomposes to $SrSi_2O_5$ plus Sr_2SiO_4 at about 11 GPa and 1000°C. This high-pressure decomposition behavior of $SrSiO_3$ is similar to that of $CaSiO_3$. The structure of the Sr_2SiO_4 phase was identified as being the Ca_2SiO_4 larnite-type, whereas the structure of the $SrSi_2O_5$ phase has not been previously determined.

In the case of $CaSiO_3$, Kanzaki et al. (1991) first reported that $CaSiO_3$ walstromite decomposes to $CaSi_2O_5$ + Ca_2SiO_4 at 10 GPa and 1f500°C and proposed the titanite ($CaSiTiO_5$) structure type as a candidate of the $CaSi_2O_5$ structure. Angel et al. (1996) found that, after pressure release to ambient conditions, the $CaSi_2O_5$ phase has a triclinic structure derived from that of titanite. A feature specific to the triclinic phase of $CaSi_2O_5$ is that it contains fivefold-coordinated silicon sites in addition to four- and six-coordinated silicon sites. Furthermore, it was shown by Angel (1997) that, under hydrostatic compression, the triclinic $CaSi_2O_5$ transforms to a monoclinic titanite phase which contains only four- and six-silicon sites.

Our powder X-ray diffraction (XRD) pattern of the $SrSi_2O_5$ phase recovered from high pressure was inconsistent not only with a titanite-type structure, but also with any known silicate mineral. From comparison of

H. Kojitani (✉) · M. Kido · M. Akaogi
Department of Chemistry, Faculty of Science,
Gakushuin University, 1-5-1 Mejiro,
Toshima-ku, Tokyo 171-8588, Japan
E-mail: hiroshi.kojitani@gakushuin.ac.jp
Tel.: +81-3-39860221
Fax: +81-3-59921029

XRD profiles among inorganic compounds with the AB_2X_5 stoichiometry, we have found that the XRD profile of $SrSi_2O_5$ phase agreed very well with that of $BaGe_2O_5$ III, reported by Ozima et al. (1982). Therefore, we have performed a Rietveld analysis of the high-pressure form of $SrSi_2O_5$ by using the crystal structure data for $BaGe_2O_5$ III as a model.

Experimental methods

The starting material was prepared from a mixture of reagent grade $SrCO_3$ and silicic acid (SiO_2·11wt% H_2O) in the molar ratio of 1:2. The mixture was compressed into a pellet and heated at 1250°C for 12 h in a furnace. The powder XRD pattern of the product could be indexed as a mixture of pseudowollastonite-type $SrSiO_3$ and SiO_2 cristobalite. The pellet was reground into powder in an agate mortar for 1 h. High-pressure and high-temperature synthesis was performed by using the Kawai-type multianvil apparatus at Gakushuin University. Tungsten carbide anvils with a truncated edge length of 5 mm were used. A MgO octahedron was used as a pressure medium. A cylindrical Pt heater was put into the octahedron with a $LaCrO_3$ sleeve and endplugs as thermal insulator. Tantalum discs were put between the $LaCrO_3$ endplugs and the sample to prevent reaction between them. Temperature was measured with a Pt/Pt–13%Rh thermocouple. A hot junction of the thermocouple was placed on the outer surface of central part of the heater. The starting material was put in the Pt heater, and kept at 16 GPa and 900°C for 1 h, then quenched isobarically. More details on the high-pressure technique employed in this study are given in Suzuki and Akaogi (1995). The composition of the recovered sample was confirmed by SEM-EDS analysis. A microscopic observation of the recovered polycrystalline sample showed that many crystals had a tabular shape (5–20 μm in diameter, 1–2 μm in thickness).

The recovered sample was crushed and ground into powder. The powdered sample was mounted on a non-reflective quartz plate using acetone. The powder XRD pattern was obtained by using a Rigaku RINT 2500V diffractometer with monochromated Cr K_α radiation (45 kV, 250 mA) at Gakushuin University. The step-scanning method was applied for data collection in a 2θ range of 10–140°. The step size and counting time were 0.02° and 20 s per step, respectively.

Rietveld analysis was made by using the RIETAN-2000 program (Izumi and Ikeda 2000). Peak profiles were fitted with the pseudo-Voigt function. The preferred orientation was corrected with the March–Dollase function (Dollase 1986). As the observed powder diffraction pattern included weak peaks of SiO_2 stishovite at 2θ = 45.6° and 70.7°, which probably originated from unreacted cristobalite in the starting material owing to the relatively low-reaction temperature, stishovite was included in the refinement as an impurity phase.

Results and discussion

Results of Rietveld analysis

The powder XRD data for $SrSi_2O_5$ are shown in Table 1. All of the observed peaks, except for those of stishovite, can be assigned to $BaGe_2O_5$ III-type $SrSi_2O_5$. The calculated d values are very consistent with the observed ones. All of their reflection indices conform to the extinction rule of the space group *Cmca*. The results of the Rietveld analysis are shown in Table 2 and Fig. 1. When atomic displacement factors for all oxygen sites were refined independently, only O2 gave a negative value. Therefore, the isotropic atomic displacement factor for O2 was fixed at zero. The weighted chi-squared value (1.05) indicates that the profile represented by refined parameters fits well with the observed XRD data. The uncertainty of each XRD data point σ, which was used in the χ^2_w examination, was estimated by applying the equation $\sigma_i = 1.33 \times n_i^{-1/2}$, where n_i is a count number at the i-th data point. The coefficient of 1.33 was based on the result of Rietveld refinement of Si, the XRD pattern of which was taken with the same experimental conditions as those for $SrSi_2O_5$.

The refined $BaGe_2O_5$ III-type structure consists of silicon–oxygen framework layers which are perpendicular to the c-axis. In a unit layer, O and Sr are stacked to form a hexagonal close packing, where a layer of O1 and O3 is sandwiched between layers of O2, O4 and Sr (Fig. 2a). On the other hand, the stacking across the unit layers is regarded as a cubic close packing. Hence, a pattern of O and Sr packing in the unit cell can be described as ABACBC. Positions of Sr in the same layer are shown in Fig. 2b by the projection on (001). Si resides in an octahedral (Si1) and a tetrahedral (Si2) sites, and Sr is in a 12-fold coordination. Using the Si–O polyhedra as building blocks, two subunit layers can be constructed in the unit layer, as shown in Figs. 2a and 3. In the subunit layer, a SiO_6 octahedron is connected by three corner-shared SiO_4 tetrahedra. The SiO_6 octahedra are linked via corners to form chains parallel to a-axis. The SrO_{12} polyhedra are positioned between the unit layers with linking each other by face sharing.

Calculated interatomic distances and angles are listed in Table 3. The average Si1–O distance (1.797 Å) shows very good agreement with average Si–O distance of 1.796 Å for SiO_6 octahedron among various high-pressure silicates (Finger and Hazen 2000). The details of the obtained SiO_6 octahedron are described as follows. The Si1–O4 distance is the longest among the Si1–O distances (0.1 Å longer than the average Si1–O distance). On the other hand, Si1–O1 and Si1–O3 distances are about 0.1 Å shorter than that of the average Si1–O distance. Most of O–Si1–O angles are close to 90° which is the one for an ideal octahedron. Only O3–Si1–O3 angle indicates about 10° larger value than the others. This is caused by the off-center of Si1 on a quadrilateral plane consisting of O3 and O4. These

Table 1 Powder XRD data for high-pressure form of $SrSi_2O_5$

h	*k*	*l*	d_{obs} (Å)	d_{calc} (Å)	Intensity
0	0	2	6.7058	6.7203	1
0	2	0	4.6398	4.6402	2
1	1	1	4.3207	4.3201	6
1	1	2	3.7738	3.7746	11
0	0	4	3.3618	3.3602	100
0	2	3	3.2232	3.2230	55
1	1	4	2.7054	2.7055	90
1	3	1	2.6139	2.6129	46
2	0	2	2.4398	2.4406	1
0	2	5	2.3264	2.3260	9
1	3	3	2.2887	2.2896	8
0	0	6	2.2401	2.2401	56
0	4	2	2.1924	2.1931	10
2	2	2	2.1604	2.1600	7
0	4	3	2.0609	2.0602	19
2	2	3	2.0329	2.0328	31
0	4	4	1.9094	1.9092	3
1	3	5	1.8920	1.8921	4
2	2	4	1.8884	1.8873	3
1	1	7	1.7699	1.7697	20
0	4	5	1.7571	1.7564	2
2	2	5	1.7391	1.7393	5
2	0	6	1.7024	1.7025	1
3	1	1		1.7024	
1	5	2	1.6931	1.6931	1
0	0	8	1.6802	1.6801	1
3	1	2	1.6626	1.6628	1
2	4	3	1.6195	1.6194	2
0	4	6	1.6119	1.6115	1
1	1	8	1.5767	1.5766	5
1	3	7	1.5569	1.5576	2
1	5	4	1.5514	1.5518	3
0	6	0	1.5469	1.5467	2
3	1	4	1.5287	1.5284	3
3	3	1	1.5115	1.5111	3
0	4	7	1.4792	1.4792	2
2	2	7	1.4691	1.4690	5
2	4	5	1.4587	1.4588	1
1	3	8	1.4217	1.4210	2
0	6	4	1.4055	1.4050	1
2	4	6	1.3729	1.3726	1
0	4	8	1.3609	1.3608	2
2	2	8	1.3530	1.3528	3
2	6	0	1.3319	1.3319	5
4	0	0	1.3101	1.3097	2
1	5	7	1.2936	1.2932	1
2	4	7	1.2878	1.2880	1
3	1	7	1.2795	1.2796	2
1	7	1		1.2794	
0	4	9	1.2559	1.2557	1
3	5	2	1.2497	1.2497	3
2	6	4	1.2382	1.2381	1

descriptions indicate that the octahedra in $SrSi_2O_5$ phase are slightly distorted. In the tetrahedra, the average Si2–O distance (1.618 Å) is almost the same within the errors as the average Si–O distance of 1.611(8) Å in coesite (Geisinger et al. 1987), a typical high-pressure silicate consisting of SiO_4 tetrahedra. However, the Si2–O1 distance is about 0.1 Å shorter than the others. The considerably large isotropic atomic displacement parameter for O1 suggests that an actual Si2–O1 distance might be longer than the value calculated by the average atomic positions. The bond valence sum (Brown and Altermatt 1985) of Si ion in the tetrahedron gives an acceptable value of 4.10 in spite of the unusually short Si2–O1 distance. The average Sr–O distance of 2.734 Å is comparable to that for cubic $SrTiO_3$ perovskite (2.76 Å : Mitchell et al. 2000), which also contains 12-coordinated Sr. As corner-linked polyhedra in this structure are not allowed to tilt, it is suggested that the adjustment of size of the divalent cation site is attained to accommodate Sr^{2+} by those deformations of SiO_4 tetrahedra and SiO_6 octahedra. This adjustment results in the difference in distances between the stacking layers of oxygen and strontium. Namely, the distance between unit layers becomes larger than the thickness of a subunit layer. This difference causes the distortion of SrO_{12} polyhedra. The distortion results in a slight deviation of the Sr position from the mean level of O2 and O4 in the same layer. The distance between unit layers is about 33% longer than the thickness of a subunit layer. In $BaGe_2O_5$ III, the difference between them is about 27%. The ionic radius ratios are 3.60 for $^{XII}Sr^{2+}/^{VI}Si^{4+}$ and 2.96 for $^{XII}Ba^{2+}/^{VI}Ge^{4+}$ using ionic radii by Shannon and Prewitt (1969). The comparison between the difference in the packing-layer thickness and the ionic ratios suggests that the relative ionic size of a divalent cation to that of a tetravalent cation may determine how much the thickness of the subunit layer should be shortened to adjust the space for the divalent cation.

Table 2 Fractional atomic coordinates and isotropic displacement factors for $BaGe_2O_5$ III-type $SrSi_2O_5$ by the Rietveld analysis

Atom	Site	*x*	*y*	*z*	B_{iso} (Å^2)
Sr	8f	0	0.3404(1)	0.0827(1)	1.35(4)
Si1	8f	0	0.6753(4)	0.1821(1)	0.81(7)
Si2	8f	0	0.0058(4)	0.1377(2)	0.30(6)
O1	8f	0	0.5148(7)	0.2480(3)	1.53(15)
O2	8f	0	0.8320(7)	0.1029(3)	0
O3	8e	1/4	0.2427(6)	1/4	0.66(15)
O4	16 g	0.2517(7)	0.0896(5)	0.0965(2)	0.42(9)

Space group *Cmca*, a = 5.2389(1) Å, b = 9.2803(2) Å, c = 13.4406(1) Å. R_{WP} = 10.80%, R_B = 4.02%, R_F = 2.28%, χ^2_w = 1.05

$$R_{WP} = \sqrt{\frac{\sum_i w_i[y_i(o)-y_i(c)]^2}{\sum_i w_i[y_i(o)]^2}} \quad R_B = \frac{\sum_k |I_k(o)-I_k(c)|}{\sum_k I_k(o)} \quad R_F = \frac{\sum_k \left|[I_k(o)]^{1/2}-[I_k(c)]^{1/2}\right|}{\sum_k [I_k(o)]^{1/2}}$$

$$\chi^2_w = \left[\sum_i y_i(o) - y_i(c)^2/\sigma_i^2\right]/(n-m)$$

Isotropic atomic displacement factor = $\exp[-B_{iso}(\sin\theta/\lambda)^2]$ y_i(o) and y_i(c) are observed and calculated intensities at profile point i, respectively. w_i is a weight for each step i. I_k(o) and I_k(c) are observed and calculated integrated intensities, respectively. n and m in the χ^2_w calculation show numbers of data and of refined parameters, respectively. B_{iso} for O2 was fixed at zero

Comparison with titanite type $CaSi_2O_5$

The titanite-type monoclinic $CaSi_2O_5$ comprises chains of corner-sharing SiO_6 octahedra running parallel to the *a*-axis. SiO_4 tetrahedra in the monoclinic $CaSi_2O_5$ connect the SiO_6 octahedral chains with corner-sharing. $BaGe_2O_5$ III-type $SrSi_2O_5$ does not contain such chains but layers consisting of SiO_6 octahedra and SiO_4

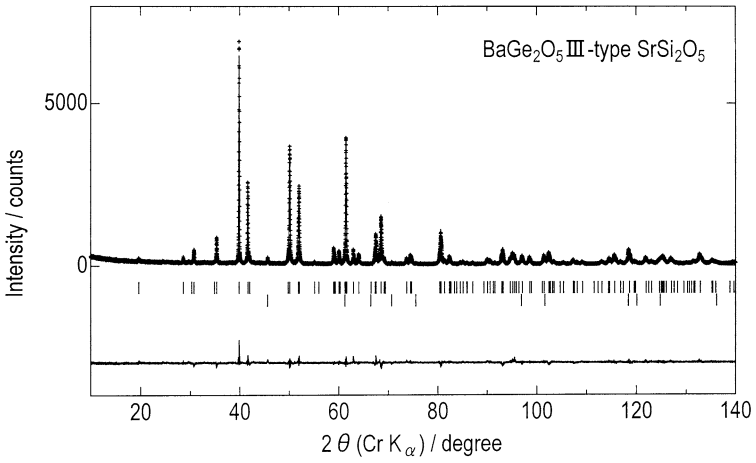

Fig. 1 Results of the Rietveld analysis of $BaGe_2O_5$ III-type $SrSi_2O_5$. *Cross* and *solid line* show observed and calculated X-ray diffraction patterns, respectively. *Vertical bars* indicate the positions of Bragg reflection for $SrSi_2O_5$ (*upper*) and SiO_2 stishovite (*lower*). The *plot at the bottom* of this figure represents the difference between the observed and calculated patterns

tetrahedra as described above. In terms of a divalent cation environment, Ca in the monoclinic $CaSi_2O_5$ has a coordination number of seven and an average Ca-O distance of 2.363 Å (Angel 1997). On the other hand, Sr in $SrSi_2O_5$ is in a 12-fold site with the average Sr–O bond length of 2.734 Å . It seems to be possible that the divalent cation site in the titanite-type structure is adjusted to accommodate a larger ion than Ca^{2+} by tilting the SiO_6 and SiO_4 polyhedra. According to Hammonds et al. (1998), however, no rigid unit mode for the titanite structure indicates that it is difficult for the Si(Ti)–O polyhedra to tilt, where the rigid unit mode is a rotational vibration mode without deformation of the polyhedra. This means Si–O polyhedra have to be deformed by shortening Si–O distances to accommodate Sr^{2+} in the site without any tilting. Since the shortened Si–O bond distance results in an energetically less stable structure, $BaGe_2O_5$ III-type structure could be favorable for $SrSi_2O_5$ due to the larger divalent cation site than that in the titanite structure. The $BaGe_2O_5$ III-type structure can be a potential candidate for high-pressure silicate containing relatively large cations such as Ba. Furthermore, as each unit layer of tetravalent cation–oxygen polyhedra is isolated by layers consisting of only divalent cations, this type of crystal structure may be expected to have practical applications (e.g., as an ionic conductor).

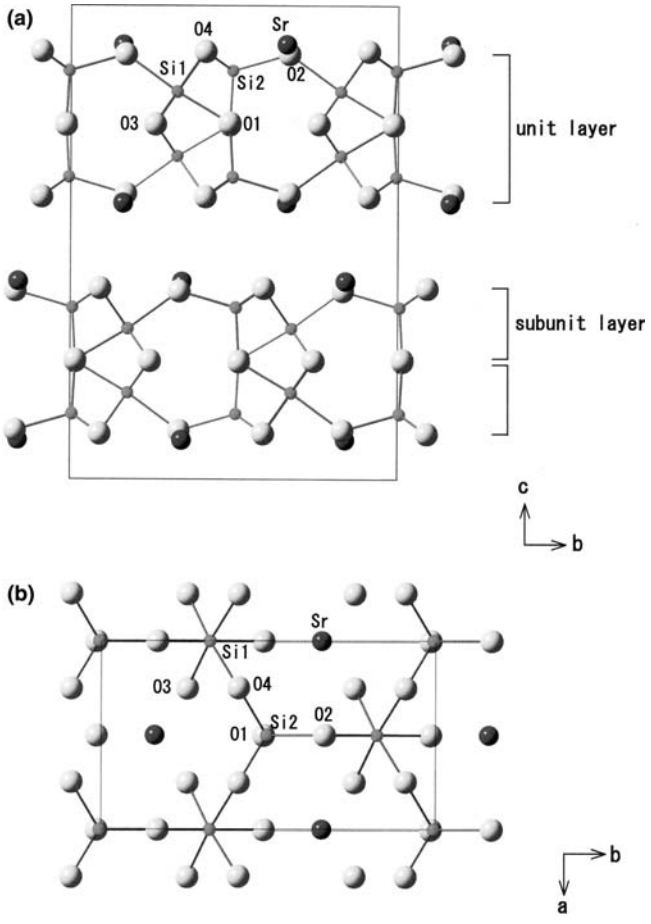

Fig. 2 Projections of the crystal structure of $BaGe_2O_5$ III-type $SrSi_2O_5$ (**a**) along the *a*-axis and (**b**) along the *c*-axis. The *rectangles* indicate a unit cell dimension

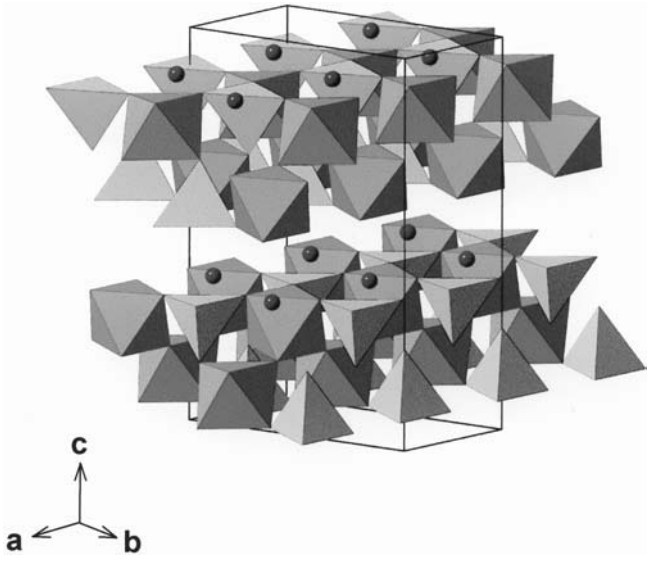

Fig. 3 Crystal structure of $BaGe_2O_5$ III-type $SrSi_2O_5$. *Tetrahedra* and *octahedra* show SiO_4 and SiO_6 polyhedra, respectively. Position of Sr is represented by *sphere*

Table 3 Interatomic distances and bond angles of $BaGe_2O_5$ III-type $SrSi_2O_5$

	Distance (Å)	O–M–O angle (degrees)
Si octahedron		
Si1–O1	1.733(7)	
–O2	1.802(6)	
–O3×2	1.714(3)	
–O4×2	1.910(4)	
Average	1.797	
O1–O3 ×2	2.488(7)	92.4(2)
O1–O4 × 2	2.513(5)	87.1(2)
O2–O3×2	2.512(4)	91.1(2)
O2–O4 ×2	2.600(6)	88.9(2)
O3–O4 × 2	2.504(5)	87.2(1)
O3–O3	2.619(1)	99.6(2)
O4–O4	2.602(8)	85.9(2)
Si tetrahedron		
Si2–O1	1.539(5)	
–O2	1.679(7)	
–O4 × 2	1.628(4)	
Average	1.618	
O1–O4× 2	2.566(5)	108.2(2)
O1–O2	2.625(8)	109.3(3)
O4–O2× 2	2.731(6)	111.4(2)
O4–O4	2.637(8)	108.2(3)
Sr polyhedron		
Sr–O1	2.749(5)	
–O2 × 2	2.635(1)	
–O2	2.963(5)	
–O3 × 2	2.756(2)	
–O4 × 2	2.661(4)	
–O4 × 2	2.681(4)	
–O4 × 2	2.814(3)	
Average	2.734	

Acknowledgements We thank Drs. Y. Inaguma, T. Katsumata and T. Kuribayashi for their helpful advises on Rietveld analysis, and also Dr. Chakhmouradian and an anonymous reviewer for constructive reviews. This study was supported in part by Grants-in-Aid from the Ministry of Education, Science and Culture, Japan, and Japan Society for the Promotion of Science.

References

Angel RJ (1997) Transformation of fivefold-coordinated silicon to octahedral silicon in calcium silicate, $CaSi_2O_5$. Am Mineral 82:836–839

Angel RJ, Ross NL, Seifert F, Fliervoet TF (1996) Structural characterization of pentacoordinate silicon in a calcium silicate. Nature 384:441–444

Brown ID, Altermatt D (1985) Bond-valence parameters obtained from a systematic analysis of the inorganic crystal structure database. Acta Cryst B 41:244–247

Dollase WA (1986) Correction of intensities for preferred orientation in powder diffractometry: application of the March model. J Appl Cryst 19:267–272

Finger LW, Hazen RM (2000) Systematics of high-pressure silicate structures. Rev Mineral Geochem 41:123–155

Fleischer JF, DeVries RC (1988) Pressure–temperature diagram for the system $SrSiO_3$. Mater Res Bull 23:609–612

Geisinger KL, Spackman MA, Gibbs GV (1987) Exploration of structure, electron density distribution, and bonding in coesite with Fourier and pseudoatom refinement methods using single-crystal X-ray diffraction data. J Phys Chem 91:3237–3244

Hammonds KD, Bosenick A, Dove MT, Heine V (1998) Rigid unit modes in crystal structures with octahedrally coordinated atoms. Am Mineral 83:476–479

Izumi F, Ikeda T (2000) A Rietveld-analysis program RIETAN-98 and its applications to zeolites. Mater Sci Forum 321–324:198–204

Kanzaki M, Stebbins JF, Xue X (1991) Characterization of quenched high pressure phases in $CaSiO_3$ system by XRD and ^{29}Si NMR. Geophys Res Lett 18:463–466

Machida K, Adachi G, Shiokawa J, Shimada M, Koizumi M, Suito K, Onodera A (1982) High-pressure synthesis, crystal structures, and luminescence properties of europium(II) metasilicate and europium(II)-activated calcium and strontium metasilicates. Inorg Chem 21:1512–1519

Mitchell RH, Chakhmouradian AR, Woodward PM (2000) Crystal chemistry of perovskite-type compounds in the tausonite-loparite series, $(Sr_{1-2x}Na_xLa_x)TiO_3$. Phys Chem Minerals 27:583–589

Ozima M (1985) Structure of high-pressure phases of barium germanium oxide, $BaGe_2O_5$. Acta Cryst C 41:1003–1007

Ozima M, Susaki J, Akimoto S, Shimizu Y (1982) The system BaO–GeO_2 at high pressures and temperatures, with special reference to high-pressure transformations in $BaGeO_3$, $BaGe_2O_5$, and $Ba_2Ge_5O_{12}$. J Sold State Chem 44:307–317

Shannon RD, Prewitt CT (1969) Effective ionic radii in oxides and fluorides. Acta Cryst B 25:925–946

Shimizu Y, Syono Y, Akimoto S (1970) High-pressure transformations in $SrGeO_3$, $SrSiO_3$, $BaGeO_3$, and $BaSiO_3$. High Temp High Press 2:113–120

Suzuki T, Akaogi M (1995) Element partitioning between olivine and silicate melt under high pressure. Phys Chem Mineral 22:411–418